The quasi-1D antiferromagnet $CsMnCl_3.2H_2O$. II. A ^{54}Mn nuclear orientation study

1991 J. Phys.: Condens. Matter 3 739

(http://iopscience.iop.org/0953-8984/3/6/010)

J. Phys.: Condens. Matter 3 (1991) 739–752. Printed in the UK

The quasi-1D antiferromagnet $CsMnCl_3 \cdot 2H_2O$: II. A ^{54}Mn nuclear orientation study

C Andrikidis†, G J Bowden‡, D H Chaplin§, W D Hutchison§, J P D Martin‡ and R J Tainsh†

† CSIRO National Measurement Laboratory, PO Box 218, Lindfield, Division of Applied Physics, NSW 2070, Australia

‡ School of Physics, University of New South Wales, Kensington, NSW 2033, Australia

§ Department of Physics, University College, Australian Defence Force Academy, Campbell ACT 2600, Australia

Received 9 August 1990

Abstract. An *in situ* ^{54}Mn nuclear orientation (NO) study of a quasi-1D antiferromagnet $CsMnCl_3 \cdot 2H_2O$ is presented and discussed. From a comparison between $CsMnCl_3 \cdot 2H_2O$, and the 3D antiferromagnet $MnCl_2 \cdot 4H_2O$, it is shown that there are significant differences in the NO behaviour of *quasi-1D and 3D antiferromagnets, in the milliKelvin regime*. For example, in zero applied field, the ^{54}Mn nuclei in $CsMnCl_3 \cdot 2H_2O$ can be cooled to much lower temperatures than those in $MnCl_2 \cdot 4H_2O$. In one crystal, a base temperature of ≈ 10 mK was reached. However, in the presence of applied magnetic fields, a strong reduction in the NO signal is observed in the quasi-1D antiferromagnet $CsMnCl_3 \cdot 2H_2O$. This is in marked contrast to $MnCl_2 \cdot 4H_2O$ in which case the application of magnetic fields leads to a rapid decrease in the nuclear spin–lattice relaxation time T_1, and hence to large NO signals. It is argued that many of the unexpected features observed in the quasi-1D antiferromagnet can be understood, at least qualitatively, in terms of both 'solitons' and a large zero-point motion of the Mn^{2+} spins. NO measurements taken in both the axial and equatorial directions reveal that there are about 12.5% spin flopped domains (solitons), in zero applied field. On the other hand, thermometric methods have been used to show that the hyperfine splitting of ^{54}Mn nuclei in $CsMnCl_3 \cdot 2H_2O$ is 356(15) MHz. This result implies that the Mn^{2+} spins in $CsMnCl_3 \cdot 2H_2O$ are characterized by a large zero-point motion of some 30%. In applied fields, it is argued that the observed reduction in the γ-ray anisotropies can be explained in terms of a substantial increase in zero-point motion, as the spin flop field is approached.

1. Introduction

In recent years, it has been shown that the nuclear spin–lattice relaxation time T_1 in antiferromagnetic $MnCl_2 \cdot 4H_2O$ can be dramatically reduced by applying a magnetic field along the easy magnetic axis (Allsop *et al* 1984). In particular, it was demonstrated that as B_{app} approaches the spin flop field B_{sf}, the spin–lattice relaxation time T_1 falls from many hours to $\leqslant 1$ s. This effect was subsequently used to cool the ^{54}Mn nuclei in $MnCl_2 \cdot 4H_2O$ down to temperatures of around 15 mK. For brevity, the technique was dubbed the 'magnon heat switch' because the nuclear spin–lattice relaxation time T_1 could be manipulated from many hours to seconds, simply by applying an external magnetic field close to B_{sf}. The technique has also been successfully used in a pulsed

0953-8984/91/060739 + 14 $03.50

NMRON study of $MnCl_2 \cdot 4H_2O$ (Le Gros *et al* 1987), and in a determination of NMR enhancement factors in the same compound (Bowden *et al* 1987).

Both $MnCl_2 \cdot 4H_2O$, and the isostructural antiferromagnet $MnBr_2 \cdot 4H_2O$, can be classified as '3D antiferromagnets' in the sense that the magnetic exchange between the Mn^{2+} ions is roughly isotropic. However, Turrell (1985) and Le Gros and co-workers (1988) have shown that the low dimensional antiferromagnetic compounds $Mn(HCOOH)_2 \cdot 4H_2O$ and tetra-methyl-manganese chlorate TMMC, possess significantly shorter nuclear spin relaxation times in zero applied field, than the isotropic 3D antiferromagnets $MnCl_2 \cdot 4H_2O$ and $MnBr_2 \cdot 4H_2O$. In this paper, it will be shown that this is also the case in the quasi-1D antiferromagnet $CsMnCl_3 \cdot 2H_2O$.

At first sight, one might expect little or no difference between $MnCl_2 \cdot 4H_2O$ and $CsMnCl_3 \cdot 2H_2O$. The Néel temperatures of these two easy axis antiferromagnetic salts are 1.62 K and 4.89 K, with spin flop transitions at 0.715(10) T and 1.68(2) T, respectively. However, as we shall see there are significant differences in their NO behaviour, in both zero and applied fields. For example, in section 4 it is shown that the largest NO signal in $CsMnCl_3 \cdot 2H_2O$ is obtained in zero applied field. This is in marked contrast to the NO signals observed in $MnCl_2 \cdot 4H_2O$. We believe that many of these differences can be traced both to the presence of solitons (sections 5 and 6), and a large zero-point motion of the Mn^{2+} spins (section 7). The theoretical arguments for a large zero-point motion in quasi-1D antiferromagnetic compounds characterized by weak crystal field anisotropy, have already been discussed in an earlier paper by Bowden and Martin (1989).

2. $CsMnCl_3 2H_2O$: previous work

The crystal structure of $CsMnCl_3 \cdot 2H_2O$ is orthorhombic *Pcca*, with four chemical units per unit cell. The cell dimensions are $a = 9.06$ Å, $b = 7.285$ Å and $c = 11.455$ Å (Jensen *et al* 1962). Below the Néel temperature the unit cell doubles in size along the *b*-axis. The magnetic space group is *P2bc'ca'* with eight Mn ions per unit cell (Spence *et al* 1969). It is also believed that this crystal is characterized by weak hydrogen bonding along the *c*-axis which gives rise to apparently perfect *ab* cleavage planes (Kopinga *et al* 1975).

In $CsMnCl_3 \cdot 2H_2O$ strong Mn^{2+}–Cl^-–Mn^{2+} superexchange along the *a*-axis, is primarily responsible for the 1D magnetic nature of this compound. The Mn^{2+} spins point alternatively along the $\pm b$-axis forming linear antiferromagnetic chains directed along the *a*-axis. The interchain interactions, in both the *b* and *c* directions, are very much weaker. Nevertheless, 3D antiferromagnetic order sets in at $T_N = 4.89$ K (Smith and Friedberg 1968 and Spence *et al* 1969).

Inelastic neutron scattering experiments have been performed on $CsMnCl_3 \cdot 2H_2O$, by Skalyo *et al* (1970). From an analysis of the dispersion curves, it was found that the exchange parameter $J(a)$ along the *a*-axis is $-0.304(3)$ meV, whereas $(J(b) + J(c)) = -0.0021(4)$ meV. As a result, the magnon dispersion curves in the *b*–*c* plane are almost 'flat'. As we shall see below in section 4 this property could have an important bearing on the magnitude of the magnon specific heat close to the spin flop field B_{sf}. Skalyo *et al* (1970) have also presented neutron scattering evidence, for the existence of 1D magnons above T_N.

Specific heat measurements, in zero applied field, have been carried out by Kopinga *et al* (1975) in the temperature range 1.1–52.0 K. In particular these authors believe that because of the weak hydrogen bonding in the *c* direction, the lattice specific heat of this

compound is more characteristic of a 2D, rather than a 3D Debye model. Following Tarasov (1963) therefore, they have interpreted the specific heat data in terms of two 2D Debye constants, parallel and perpendicular to the *ab* layers respectively, together with an interlayer coupling constant ϑ_3.

To date no specific heat measurements have been made in the presence of an applied magnetic field. However, Takeda *et al* (1982) have made a specific heat study of the quasi-1D antiferromagnet $(CH_3)_3NHMnX_3 \cdot 2H_2O$ where $X = Cl$, Br. In particular, their results (0.5–1.1 K) reveal a dramatic increase in the magnon specific heat, in the presence of a spin flop field directed along the easy *b*-axis. This is associated with

(i) the reduction in the magnitude of the magnon energy gap, which goes to zero at the spin–flop field, and

(ii) almost flat excitation curves $E(k)$ against k in two directions.

It should also be noted that antiferromagnetic Mn^{2+} resonance experiments on $CsMnCl_3 \cdot 2H_2O$, have been carried out by Nagata and Tazuke (1970). From an analysis of the applied field dependence of the resonances at 1.5 K, they found $B_c = 0.045$ T and $B_a = 0.144$ T for the orthorhombic magnetic anisotropy fields, respectively. These results can be compared with the calculated anisotropy fields $B_{dip}(c) = 0.045$ T and $B_{dip}(a) = 0.095$ T arising from the dipolar interactions between the Mn^{2+} spins (Botterman *et al* 1969). The *c*-axis results are seen to be in good agreement with each other indicating that dipolar interactions could be responsible for the magnetic anisotropy field B_c. However, Nagata and Tazuke (1970) argue that the difference between the *a*-axis results is probably due to the presence of a single-ion crystal field interaction $D/g\mu_B \cong 0.01$ T. Nevertheless it would appear that dipole–dipole interactions, particularly between the 1D chains, could be important in $CsMnCl_3 \cdot 2H_2O$.

Finally, direct evidence of coupling between the magnons and phonons in $CsMnCl_3 \cdot 2H_2O$ has been presented by Weiyi Jia *et al* (1981) who found magnon sidebands present in the optical spectra. These sidebands persist above T_N, which suggests that the phonons are interacting with 1D magnons travelling along the *a*-axis, where strong exchange is present.

3. Experimental details

Single crystals of $CsMnCl_3 \cdot 2H_2O$, doped with ^{54}Mn, were grown from a saturated aqueous solution containing equi-molar concentrations of CsCl and $MnCl_2 \cdot 4H_2O$. Small pink orthorhombic crystals were produced 5 mm × 3 mm × 0.5 mm in size. The axes of the crystals were readily identified by eye (Jensen *et al* 1962) since the *c*-axis and *a*-axis are parallel to the shortest and longest crystal dimensions, respectively. Best crystal growth was achieved by

(i) setting the temperature of the solution at 30 °C, and

(ii) using a small opening in the lid of the 25 ml beaker, to slow evaporation of water.

The single crystals of $CsMnCl_3 \cdot 2H_2O$ were attached to the end of a Cu finger using Balzers silver paint. Silver paint was found to be very effective in reducing the thermal contact resistance between the sample and the cooled copper rod (Allsop *et al* 1984). The copper finger was subsequently screwed into the bottom of an Oxford Instruments dilution unit and cooled to a temperature of 6 mK.

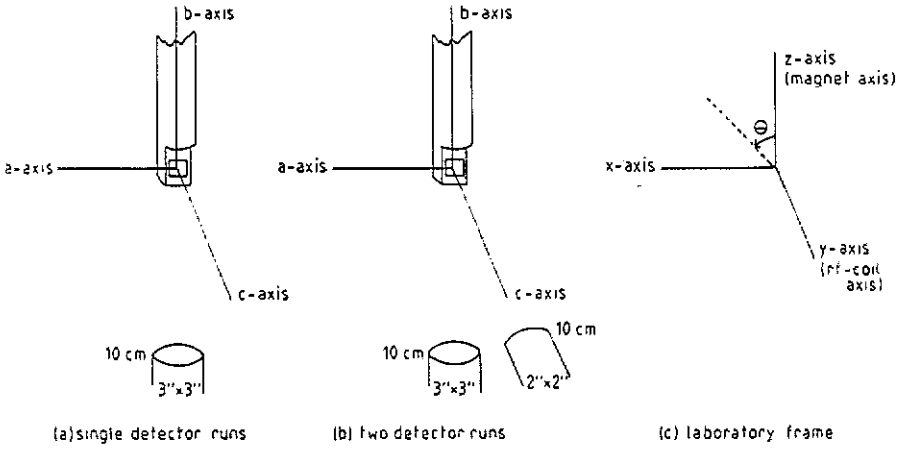

Figure 1. Orientation of the $CsMnCl_3 \cdot 2H_2O$ crystal and NaI detectors with respect to the laboratory frame of reference.

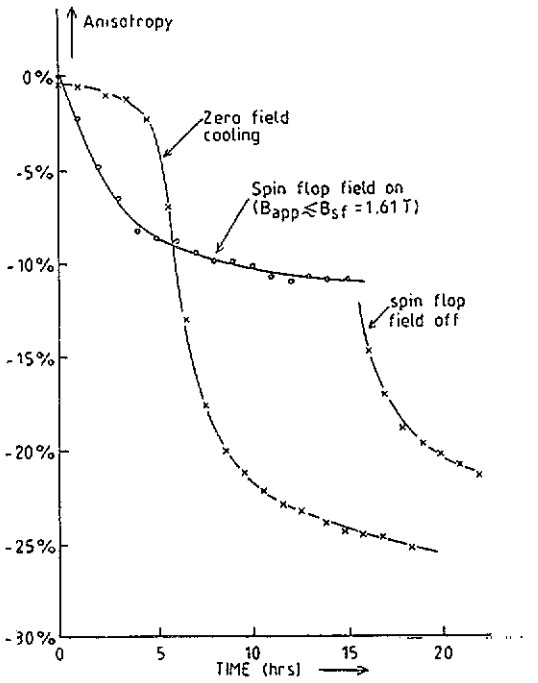

Figure 2. Axial γ-ray anisotropy of the ^{54}Mn 0.8348 MeV transition in $CsMnCl_3 \cdot 2H_2O$ below 300 mK (NML, CSIRO).

In the early set of experiments carried out in the National Measurement Laboratory (NML) CSIRO, the crystal was mounted with the easy *b*-axis in the vertical position, parallel to the axial field of a 0–3.5 T superconducting magnet. The ^{54}Mn 0.8348 MeV γ-rays were detected using NaI detectors placed as shown in figure 1. In a later set of

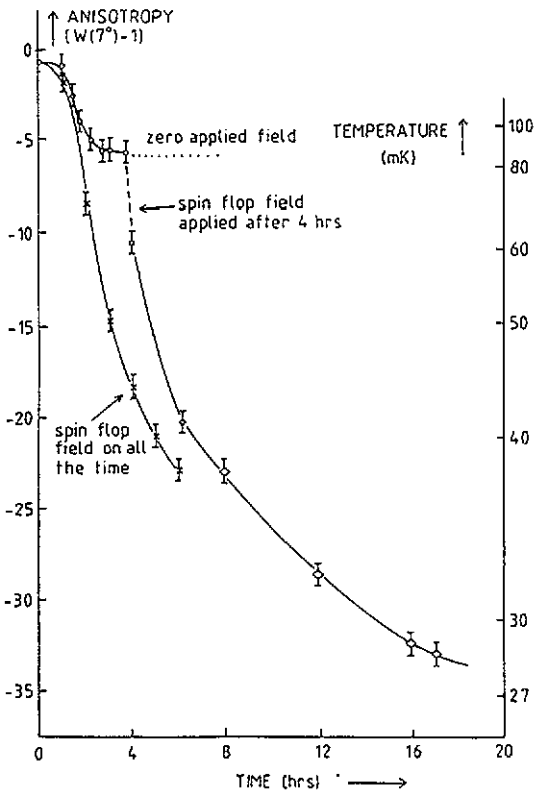

Figure 3. Near-axial γ-ray anisotropy of the ^{54}Mn 0.8348 MeV transition in $MnCl_2 \cdot 4H_2O$ below 300 mK (NML, CSIRO).

experiments carried out at the University College, Australian Defence Force Academy (ADFA), the crystal was mounted in essentially the same geometry, however this time the ^{54}Mn γ-rays were analysed using Ge detectors. Altogether some nine crystals were examined, five at the CSIRO and four at ADFA.

4. Nuclear orientation results

In the first set of experiments, carried out in the CSIRO, the ^{54}Mn 0.8348 MeV axial γ-ray anisotropies, in both $CsMnCl_3 \cdot 2H_2O$ and $MnCl_2 \cdot 4H_2O$ were obtained as a function of elapsed time (cooling curves). In obtaining the NO data, the starting time was set when the temperature of the mixing chamber passed below 300 mK, as measured by a Ge resistance thermometer. The results can be seen in figures 2 and 3, respectively.

The 0.8348 MeV γ-ray anisotropy pattern was analysed using the standard formula (e.g. Steffen and Alder 1975).

$$W(\vartheta) = 1 + \sqrt{(2I+1)}(A_2\rho_0^2 Q_2 P_2 \cos\vartheta + A_4\rho_0^4 Q_4 P_4 \cos\vartheta) \qquad (1)$$

where $W(\vartheta)$ is the normalized cold count, $A_2 = -2\sqrt{3}/7$ and $A_4 = -2\sqrt{22}/21$, Q_2 and

Q_4 are solid angle correction factors, ρ_0^2 and ρ_0^4 are the Fano statistical tensors which describe the orientation of the nuclear ensemble, and the remaining symbols possess their usual meanings.

From a comparison of the NO data shown in figures 2 and 3, it will be observed that there are significant differences in the cooling behaviour of the quasi-1D and 3D antiferromagnetic salts in question. In zero applied field the ^{54}Mn nuclei in $CsMnCl_3 \cdot 2H_2O$ show little tendency to orientate in the first four hours. By way of contrast the ^{54}Mn nuclei in $MnCl_2 \cdot 4H_2O$ quickly develop -5.5% anisotropy in the axial γ-ray emission pattern. However, after four hours, with the Cu finger now well below 50 mK, the ^{54}Mn nuclei in $CsMnCl_3 \cdot 2H_2O$ begin to display orientation. Thereafter a steady decrease in the γ-ray anisotropy is observed, and after twenty hours a value of -25% anisotropy is reached. Once again this is in marked contrast to ^{54}Mn in $MnCl_2 \cdot 4H_2O$ which shows little tendency to cool below 90 mK (-5% γ-ray anisotropy) in zero applied field.

There are also marked differences between quasi-1D and 3D antiferromagnets in applied magnetic fields. In $MnCl_2 \cdot 4H_2O$, the nuclear spin cooling rate in $MnCl_2 \cdot 4H_2O$ is maximized by setting the applied field just below the spin flop field of 0.715(5) T (Allsop *et al* 1984). This is illustrated in figure 3 where it will be observed that the ^{54}Mn spin temperature in $MnCl_2 \cdot 4H_2O$ reaches 38 mK in about 6 h. The situation, however, in $CsMnCl_3 \cdot 2H_2O$ is quite different. The measured axial γ-ray anisotropy, in an applied field of 1.61 T, can also be seen in figure 2. This field is just below the spin flop field of 1.68(2)T determined during the course of this work (see section 8). From a comparison of figures 2 and 3 it will be seen that the ^{54}Mn nuclei, in both salts, show orientation when

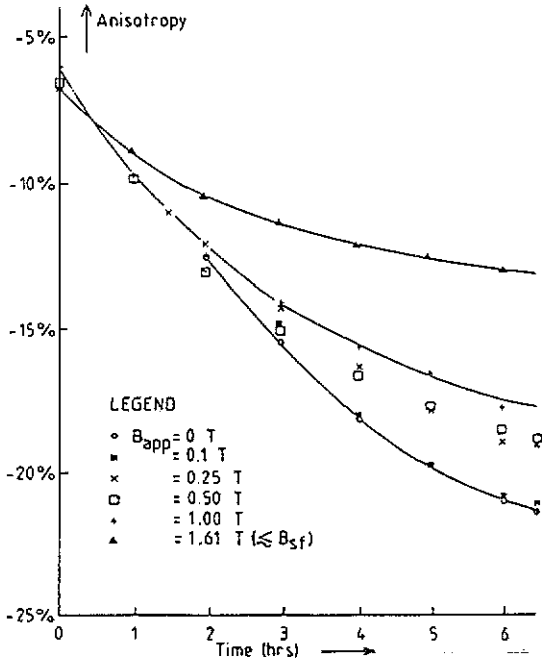

Figure 4. Axial γ-ray anisotropy of the ^{54}Mn 0.8348 MeV transition in $CsMnCl_3 \cdot 2H_2O$, in different applied fields (NML, CSIRO).

the mixing chamber falls below 100 mK, as expected. In both compounds the energy gap in their respective magnon dispersion curves is close to zero. Consequently, the nuclear-magnon relaxation rate should be very rapid (Allsop *et al* (1984). See also Beeman and Pincus (1968), Freyne (1974) and Pacquette *et al* (1975)). However, in the case of $CsMnCl_3 \cdot 2H_2O$, in a magnetic field close to B_{sf}, an effective ^{54}Mn γ-ray anisotropy limit of -12% is reached after 20 h, cf -25% in zero applied field. Note also that, if the magnetic field is subsequently removed, the ^{54}Mn nuclei in $CsMnCl_3 \cdot 2H_2O$ show an immediate increase in orientation, at a rate which is practically identical to the zero-field result, but now displaced in time.

At first sight it might be thought that the difference in the spin-flop cooling behaviour could be due to differences in their respective magnon specific heats. As noted earlier, quasi-1D antiferromagnets are characterized by flat almost dispersionless excitation curves in two directions. Consequently, in the presence of a zero energy gap, the specific heat C_M in a quasi-1D antiferromagnet should be very large. Thus the reduced NO signal (-12%) observed in $CsMnCl_3 \cdot 2H_2O$, could simply reflect the large increase in its specific heat, near or at the spin flop transition.

To test this idea, NO measurements were carried out in various applied magnetic fields 0–1.61 T. If the specific heat hypothesis is correct, the observed NO data should change rather abruptly near the spin-flop field transition. In practice the magnon specific heat depends rather sensitively on the size of the magnon energy gap $\hbar\omega(0)$ $(=g\mu_B(B_{sf} - B_{app}))$ through the exponential term $\exp(-\hbar\omega(0)/kT)$ (see for example Akhiezer *et al* (1968), and Takeda *et al* (1982)).

The experimental results for applied fields of 0, 0.1, 0.25, 0.5, 1.0 and 1.61 T are summarized in figure 4. It will be observed that even modest applied fields have an appreciable effect on the observed ^{54}Mn NO data in $CsMnCl_3 \cdot 2H_2O$. This result therefore strongly suggests that a mechanism other than specific heats is at play. Two possible mechanisms, solitons and large zero-point motion, are discussed in sections 5–8 below.

5. Solitons

De Groot and de Jongh (1986) have argued that many properties of quasi-1D antiferromagnets can be interpreted in terms of solitons. From the NO point of view, a soliton can be visualized as a small amount of spin flop phase travelling along a linear antiferromagnetic chain. Conversely, in fields above B_{sf}, solitons give rise to small amounts of antiferromagnetic phase, in the predominantly spin flopped material.

It is clear therefore, that quite apart from relaxation considerations, the presence or otherwise of solitons should have a pronounced effect on the ^{54}Mn γ-ray emission pattern. Experiments were therefore carried out using two detectors, in an attempt to confirm the existence, or otherwise, of solitons in $CsMnCl_3 \cdot 2H_2O$. However, before presenting these results a few theoretical comments are in order.

In fields well below the spin flop field B_{sf} de Groot and de Jongh (1986), have argued that the density of solitons can be gauged using a dilute gas analogy. Explicitly

$$n_s = (2\sqrt{2}/d_s\sqrt{\pi})(E_s/k_BT)^{1/2} \exp(-E_s/k_BT) \tag{2}$$

where n_s is the soliton density at temperature T, d_s is the width of the soliton, and E_s is

the energy of the soliton. Using an effective anisotropy model, de Groot and de Jongh (1986) estimate the energy of the soliton to be

$$E_s = 4|D_{\text{eff}}\tilde{J}|^{1/2} \tag{3}$$

where $\tilde{J} = JS(S+1)$, D_{eff}, the effective anisotropy parameter, is given by

$$D_{\text{eff}} = DS(S+1)(1 - B_{\text{app}}^2/B_{\text{sf}}^2) \tag{4}$$

and D is the single-ion magnetic anisotropy parameter, which is related to the anisotropy field B_A by the relationship

$$B_A = 4|D|/g\mu_B. \tag{5}$$

In $CsMnCl_3 \cdot 2H_2O$, using the exchange field $B_{EX} = 23$ T (Butterworth *et al* 1973), we estimate B_A to be 0.061 T and therefore $E_S \approx 2.79$ K in zero applied field. Consequently, at 50 mK the density of solitons should be negligible. In this regard, it is perhaps worth noting that de Groot and de Jongh (1986) have only used the soliton gas model to fit experimental data obtained above 1 K. At these temperatures, of course, the density of solitons is finite and will play a role in minimizing the free energy $F = U - TS$ of the system. However as $T \rightarrow 0$ K, the density of solitons, and their specific heat, should fall rapidly.

It would appear therefore that in zero applied field, in the mK region, $CsMnCl_3 \cdot 2H_2O$ should be essentially free of solitons. However, this will not be the case if the solitons are immobile, i.e. pinned domain walls. Alternatively, it is possible that the lifetime of a soliton at mK temperatures is excessively long. Solitons obey a wealth of conservation laws (see for example Davydov 1986). Thus it is conceivable that solitons created in abundance at higher temperatures become 'trapped' as the temperature of the crystal falls to mK regions. If this hypothesis is correct, then we have a ready explanation of the lack of NO signal in the first 4 h. For an antiferromagnet containing say 50% flopped domains, the NO signal will be close to zero even if the nuclei are 'cold'. Thus the apparent rapid increase of the NO signal after the first 4 h, is not due to a sudden decrease in the spin–lattice relaxation time T_1, but rather to the slow decay of solitions, perhaps via the hyperfine interaction $AI \cdot S$, as they try to come into thermal equilibrium with the lattice.

An increase in solitons, brought about by the presence of applied magnetic fields, can also be used to provide an explanation of the reduced NO signals shown in figure 4. The energy required to create a soliton decreases with increasing magnetic field (see equations (4) and (5)). This will lead to an increase in the density of solitons (see equation (2)), and hence to a reduction in the NO signal.

The above arguments suggest, therefore, that the thermal estimates of n_s may be invalid in the mK regime. Additional experiments were therefore carried out, using two NaI detectors in the axial and equatorial positions as shown in figure 1(*b*), in an attempt to confirm the presence or otherwise of solitons. The results are summarized in figure 5. In the following sections, it will be argued that the NO results shown in figures 2, 4 and 5, can only be fully understood in terms of a large field-dependent zero-point motion.

6. Solitons or zero-point motion?

If we assume that the Fano statistical tensors ρ_0^2 and ρ_0^4 are dominated by the magnetic hyperfine splitting, as for the ^{54}Mn nuclei in $MnCl_2 \cdot 4H_2O$, then it is easily shown using

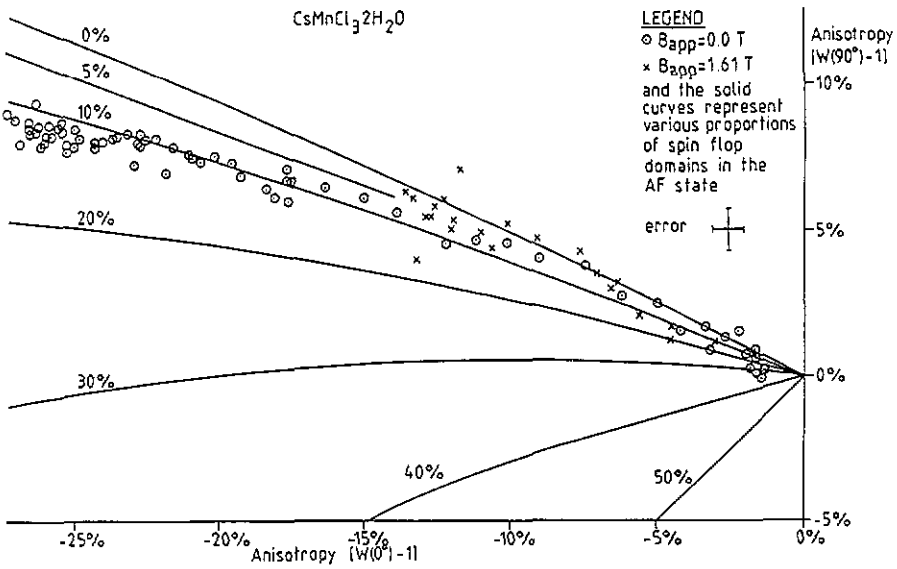

Figure 5. Axial versus equatorial γ-ray anisotropy of the ^{54}Mn 0.8348 MeV transition in $CsMnCl_3 \cdot 2H_2O$ (NML, CSIRO).

equation (1), that the γ-ray anisotropy pattern $W(\vartheta) - 1$, for the ^{54}Mn 0.8348 MeV transition, for $\vartheta = 0°$ and 90°, is given by

$$W(0°) - 1 = -\sqrt{7}(0.463\rho_0^2 + 0.357\rho_0^4) \tag{6}$$

$$W(90°) - 1 = \sqrt{7}(0.2395\rho_0^2 - 0.150\rho_0^4) \tag{7}$$

where we employed the solid angle correction factors Q_2 and Q_4 given by Yates (1965). Consequently, if we assume that the solitons can be represented by spin-flopped domains orientated at 90° (by calculation we estimate 87.7°), then the measured γ-ray anisotropy for both the axial and equatorial detectors can be written in the form

$$W_{obs}(0°) - 1 = (1 - \alpha)(W(0°) - 1) + \alpha(W(90°) - 1) \tag{8}$$

$$W_{obs}(90°) - 1 = (1 - \alpha)(W(90°) - 1) + \alpha(W(0°) - 1) \tag{9}$$

respectively, where α represents the proportion of spin-flop domains present in the sample. Note that this very simple model does not take into account any gradual changes in spin direction on traversing a given soliton. Thus conclusions based on equations (8) and (9) must be viewed as 'first approximations'.

The zero-field cool-down NO data, obtained using two detectors are summarized in figure 5. It will be observed from a comparison of the experimental data, and the theoretical curves for various values of α, that the best fit is obtained when $\alpha = 12.5\%$, i.e. 12.5% of spin flopped domains (solitons) in the predominantly antiferromagnetic crystal. Presumably, these solitons introduce energy states into the 'forbidden' magnon energy gap, which in turn give rise to a decrease in the nuclear spin relaxation rate T_1 (see Kosevich 1986 and Gladkov 1984).

The axial and equatorial NO data, obtained in a field of 1.61 T, can also be seen in figure 5. Unfortunately, it is difficult to obtain a reliable estimate of α from this data

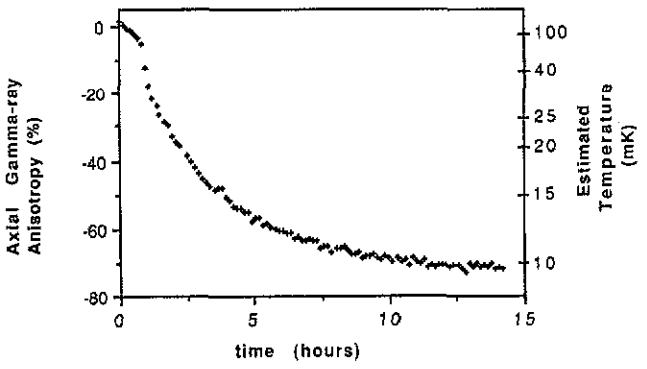

Figure 6. Axial γ-ray anisotropy of the ^{54}Mn 0.8348 MeV transition in $CsMnCl_3 \cdot 2H_2O$ below 300 mK in zero applied field (ADFA). The temperature scale on the right is based on a magnetic hyperfine splitting of 356 MHz.

because the measured γ-ray anisotropies are so small. Nevertheless, it woud appear that $0 \leqslant \alpha \leqslant 15\%$ i.e. no net increase in solitons. This figure is far from the anticipated increase of say 30%, which would be easily detectable. Thus our earlier conjecture, concerning the increase in soliton population induced by the presence of magnetic fields, is unlikely to be correct. In the following section, an alternative explanation based on the existence of a large zero-point motion is presented and discussed. In particular, it is shown that in zero applied field, the Mn^{2+} ion is characterized by a near 30% reduction in the magnitude of the Mn magnetic hyperfine field.

7. Thermometric determination of the ^{54}Mn magnetic hyperfine field in $CsMnCl_32H_2O$

In the second set of experiments carried out at ADFA, much of the earlier work presented above was confirmed. Specifically, in three of the four crystals examined the lowest ^{54}Mn γ-ray axial anisotropy reached in zero field was -25%. The figure of 12.5% spin flop domains in zero applied field was also confirmed. However, in one crystal a much greater NO signal of -72% was achieved. The measured axial anisotropy as a function of time for this particular crystal can be seen in figure 6.

The difference in the ultimate NO signal reached in this particular crystal, and that obtained in all the other runs, is difficult to explain. In both cases the crystals were attached to the cold finger with the same silver paint in an identical manner i.e. with the flat a–b plane parallel to the cold finger. It is possible that the marked difference in the zero-field cooling curves of $CsMnCl_3 \cdot 2H_2O$, shown in figures 3 and 6, may be due to the tendency of the crystals to cleave in the a–b plane. Kopinga *et al* (1975) have remarked that $CsMnCl_3 \cdot 2H_2O$ consists of weakly coupled layers, perpendicular to the c-axis. Thus it is possible that a substantial temperature difference exists along the c-axis, with only the ^{54}Mn nuclei close to the cold finger showing orientation. Later physical examination of the crystals indeed showed indications of cleavage, presumably brought about by thermal strain. This suggests therefore that small thin crystals should be used to minimize Kapitza boundary and cooling problems brought about by cleavage planes. However, our experience has shown that even the adoption of this strategy does not guarantee success. Furthermore, an experiment with a small thin crystal attached to the

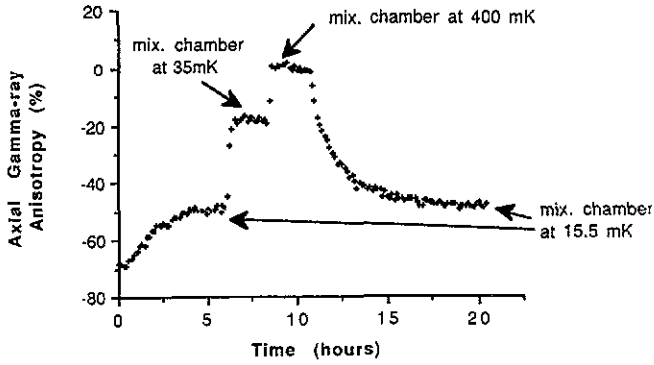

Figure 7. Axial γ-ray anisotropy of the ^{54}Mn 0.8348 MeV transition in $CsMnCl_3 \cdot 2H_2O$ at a temperature of 15.5(5) mK in zero applied field (ADFA).

copper rod with the *a–c* plane, rather than the *a–b* plane, also gave a maximum NO signal of only −25%.

Nevertheless, the large axial γ-ray anisotropy shown in figure 6 suggests that this particular crystal is characterized by very few solitons, and is in excellent thermal contact with the cold finger. In view of these circumstances, an attempt was made to determine the magnetic hyperfine splitting by thermal methods. The results are summarized in figure 7 where it will be observed that a steady state NO signal of 50% at 15.5(5) mK, as determined by an ^{125}Sb in Fe thermometer, was obtained regardless of whether the 15.5 mK temperature was approached from below (7 mK → 15.5 mK) or above (400 mK → 15.5 mK). From an analysis of this result we deduce

$$g_N \mu_N B_{hyp}/h = 356(15)\ \text{MHz} \tag{10}$$

which is some 30% below the magnetic hyperfine splitting of about 500 MHz observed in the 3D antiferromagnet $MnCl_2 \cdot 4H_2O$ (Allsop *et al* 1984). We conclude that the Mn^{2+} spins in the quasi-1D antiferromagnet are characterized by a zero-point motion of about 30%, in good agreement with the RPA prediction of Bowden and Martin (1989). (A similar estimate was also obtained at the CSIRO from crystals at higher temperatures.) The temperature scale shown in figure 6 is based on the magnetic hyperfine splitting given above. A more accurate temperature scale must await NMRON experiments. Note that the reduced hyperfine field of equation (10) implies that a lower temperature (and hence a longer cool-down time) is required, to bring about appreciable nuclear orientation in $CsMnCl_3 \cdot 2H_2O$.

Finally, we suggest that the reduction in the NO γ-ray anisotropies observed in applied magnetic fields (see figure 4) is due primarily to an increase in zero-point motion, and hence to a reduction in the ^{54}Mn hyperfine field. As noted by Bowden and Martin (1989), the zero-point motion will increase as the effective anisotropy parameter D_{eff} falls with increasing magnetic field (see for example figures 2 and 9 of their paper). Thus the final γ-ray anisotropy observed in a field of 1.61 T, is dictated, primarily, by a reduced magnetic hyperfine splitting, which we estimate to be about 200 MHz.

8. The spin-flop transition in the mK regime

Butterworth *et al* (1973) have made a detailed study of the phase transitions in $CsMnCl_3 \cdot 2H_2O$, in the temperature range 1–6 K. From their results, they conclude that the extrapolated value of the spin flop field B_{sf} is 1.61 T, at $T = 0$ K.

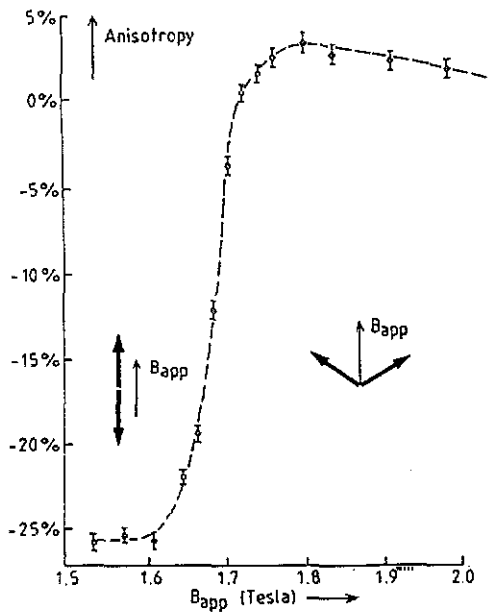

Figure 8. The spin flop transition in $CsMnCl_3 \cdot 2H_2O$ (NML, CSIRO).

The determination of the spin flop field using an initial NO signal of -25%, is shown in figure 8. We find $B_{sf} = 1.68(2)$ T in reasonable agreement with Butterworth *et al* (1973). As with $MnCl_2 \cdot 4H_2O$, no hysteretic effects were observed, within experimental error, on transversing backwards and forwards through the spin flop field, This suggests, therefore, that the spin flop transition is second-order in nature, proceeding perhaps through the formation of mixed antiferromagnetic and spin flop domains (see for example King and Pacquette 1973). In addition, de Groot and de Jongh (1986) have argued that the spin flop phase transition in quasi-1D antiferromagnets should be 'continuous', over a fairly wide magnetic field range. Using the NO data we have estimated the widths of the transitions, using 10% and 90% limits, for both $MnCl_2 \cdot 4H_2O$ and $CsMnCl_3 \cdot 2H_2O$. We find $\Delta B_{sf} = 0.018(2)$ T and 0.082(6) T, respectively. Clearly, the spin flop transition in $CsMnCl_3 \cdot 2H_2O$ is broader than that observed in $MnCl_2 \cdot 4H_2O$ by a factor of about five. Similar broadening has also been observed in the quasi-1D antiferromagnet K_2FeF_5 by Gupta *et al* (1979), using Mössbauer techniques.

Finally, in the previous section it was argued that the ^{54}Mn magnetic hyperfine splitting is significantly reduced in the presence of a magnetic field. In practice, such changes in the magnetic hyperfine field are not observed as the spin flop transition is traversed, because the nuclear spin-lattice relaxation times T_1, in both zero and applied fields at base temperatures, are excessively long. Thus the populations of the nuclear levels remain undisturbed across the spin flop transition, at least during the time scale (2 h) of the experiment. At higher temperatures, however, considerable hysteresis was observed in the NO signal, reflecting the marked differences in nuclear spin–lattice relaxation times T_1 in zero and applied fields.

9. Discussion and conclusions

At high temperatures, of around 80 mK, the nuclear relaxation time in both $CsMnCl_3 \cdot 2H_2O$ and $MnCl_2 \cdot 4H_2O$ decreases when the energy gap in the magnon

dispersion curve is reduced to zero, as expected. However, at lower temperatures there are significant differences in the NO behaviour of quasi-1D and 3D antiferromagnetic salts. In zero applied field, for example, the ^{54}Mn nuclei in $CsMnCl_3 \cdot 2H_2O$ can be cooled to much lower temperatures than those in $MnCl_2 \cdot 4H_2O$. The reduced spin–lattice relaxation times observed in quasi-1D antiferromagnets, is presumably due to the presence of solitons, which introduce energy states into the 'forbidden' magnon energy gap (Kosevich 1986).

Experimental evidence for the existence of solitons (or pinned domain walls) in the mK regime, has also been presented and discussed. NO experiments using axial and equatorial detectors have been used to show that, in zero applied field, there are around 12.5% spin flop domains in the nominally antiferromagnetic phase. However, in applied magnetic fields the observed reduction in the γ-ray anisotropy cannot be explained in terms of a corresponding increase in solitons.

Thermometric methods have also been used to show that the ^{54}Mn magnetic hyperfine splitting in $CsMnCl_3 \cdot 2H_2O$ is 356(15) MHz, cf 500.38(1) MHz observed in $MnCl_2 \cdot 4H_2O$ by Allsop *et al* (1984). This constitutes a zero-point motion of some 30%. This figure is in good agreement with the RPA calculations of Bowden and Martin (1989).

The reduction in the NO γ-ray anisotropy observed in applied magnetic fields has been tentatively ascribed to an increase in the zero-point motion of the Mn^{2+} spins. For example, using the data shown in figures 2 and 7, we estimate that the ^{54}Mn hyperfine splitting approaches 200 MHz, in a field of 1.61 T. Note that this decrease in hyperfine field will not be observed in traversing the spin flop transition, adiabatically.

Clearly it would be advantageous to carry out NMRON experiments on $CsMnCl_3 \cdot 2H_2O$ in order to establish the hyperfine parameters of the ^{54}Mn nucleus with more precision. However, a calculation reveals that the NMR enhancement factor η for the ^{54}Mn nuclei in $CsMnCl_3 \cdot 2H_2O$ is about -0.19, much lower than the estimate of $+24.9$ obtained for $MnCl_2 \cdot 4H_2O$. This suggests, therefore, that NMRON experiments in the quasi-1D antiferromagnet $CsMnCl_3 \cdot 2H_2O$ are likely to be difficult.

Acknowledgments

Both GJB and DHC would like to thank the Australian Research Grants Scheme and the University of New South Wales for financial assistance during the course of this work. JPDM would like to thank the Commonwealth Department of Education for a Postgraduate Research Award.

References

Akhiezer A I, Bar'yakhtar V G and Petetminskii S V 1968 *Spin Waves* (Amsterdam: North-Holland)
Allsop A L, de Araujo M, Bowden G J, Clark R G and Stone N J 1984 *J. Phys. C: Solid State Phys.* **17** 915
Beeman D and Pincus P 1968 *Phys. Rev.* **166** 359
Botterman A C, de Jonge W J M and de Leeuw P 1969 *Phys. Lett.* **30**A 150
Bowden G J and Martin J P D 1989 *J. Phys.: Condens. Matter* **1** 179
Bowden G J, Martin J P D, Stone N, Andrikidis C and Tainsh R J 1987 *J. Phys. C: Solid State Phys.* **20** 4657
Butterworth G J, Woollam J A and Aron P 1973 *Physica* **70** 547
Davydov A S 1986 *Solitons* (*Modern Problems in Condensed Matter Physics*) vol 17 (Amsterdam: North-Holland)
De Groot H J M and de Jongh L J 1986 *Physica* B **141** 1
Freyne F 1974 *Phys. Rev.* B **9** 4824

Gladkov S O 1984 *Sov. Phys.–Solid State* **26** 1921
Gupta G P, Dickson D P E and Johnson C E 1979 *J. Phys. C: Solid State Phys.* **12** 2411
Jensen S J, Andersen P and Rasmussen S E 1962 *Acta Chem. Scand.* **16** 1890
King A R and Pacquette D 1973 *Phys. Rev. Lett.* **30** 662
Kopinga K, de Neef T and de Jonge W J M 1975 *Phys. Rev.* B **11** 2364
Kosevich A M 1986 *Solitons* (*Modern Problems in Condensed Matter Physics 17*) (Amsterdam: North-Holland)
Kotlicki A and Turrell B G 1986 *Phys. Rev. Lett.* **56** 773
Le Gros M, Kotlicki A and Turrell B G 1987 *Hyperfine Interact.* **36** 161
Le Gros M, Kotlicki A and Turrell B G 1988 *Hyperfine Interact.* **43** 311
Miedema A R, Wielinga R F and Huiskamp W J 1965 *Physica* **31** 835
Nagata K and Tazuke Y 1970 *Phys. Lett.* **31A** 293
Paquette D, King A R and Jaccarino V 1975 *Phys. Rev.* B **11** 1193
Skalyo Jr J, Shirane G, Friedberg S A and Kobayashi H 1970 *Phys. Rev.* B **2** 4632, 1310
Smith T and Friedberg S A 1968 *Phys. Rev.* **176** 660
Spence R D, de Jonge W J M and Rama Rao K V S 1969 *J. Chem. Phys.* **51** 4694
Steffan R M and Alder K 1975 *The Electromagnetic Interaction in Nuclear Spectroscopy* (Amsterdam: North Holland) ch 12
Takeda K, Koike T, Harada I and Tonegawa T 1982 *J. Phys. Soc. Japan.* **51** 85
Tarasov V V 1963 *New Problems in the Physics of Glass* (London: Oldbourne)
Turrell B G 1985 *Hyperfine Interact.* **22** 187
Weiji Jia, Strauss E and Yen W M 1981 *Phys. Rev.* B **23** 6075
Yates M J L 1965 α, β, γ-*ray Spectroscopy* vol 2 (Amsterdam: North-Holland)